Heatwaves recurrence aggravates thermal stress in the surfgrass *Phyllospadix scouleri*

Authors: Manuel Vivanco-Bercovich[a#], Jose Miguel Sandoval-Gil*[a#], Paula Bonet-Meliá[a], Alejandro Cabello-Pasini[a], Raquel Muñiz-Salazar[a,b], Leonardo Ruiz Montoya[a], Nadine Schubert[c], Lázaro Marín-Guirao[d], Gabriele Procaccini[e], Alejandra Ferreira-Arrieta[a]

[a]Universidad Autónoma de Baja California (UABC), Instituto de Investigaciones Oceanológicas (IIO), Marine Botany Research Group, Ensenada, Baja California, México

[b]Universidad Autónoma de Baja California (UABC), Escuela de Ciencias de la Salud, Ensenada, Baja California, México

[c]CCMAR – Center of Marine Sciences, University of Algarve, Faro, Portugal.

[d]Instituto Español de Oceanografía (IEO), Centro Oceanográfico de Murcia, Seagrass Ecology Group, C/Varadero s/n, 30740 San Pedro del Pinatar, Murcia, Spain.

[e]Stazione Zoologica Anton Dohrn, Department of Integrative Marine Ecology, Villa Comunale, Naples, Italy.

# These authors contributed equally to the manuscript.

***Corresponding author:** Jose Miguel Sandoval Gil, Universidad Autónoma de Baja California (UABC), Instituto de Investigaciones Oceanológicas, Carretera Ensenada-Tijuana No. 3917, Fraccionamiento Playitas C.P. 22860 en Ensenada, Baja California, México. Tel: +52 1 646 138 9598

jmsandovalgil@gmail.com

Orcid ID: **0000-0001-8973-0306**

Preprint not peer reviewed

This preprint research paper has not been peer reviewed. Electronic copy available at: https://ssrn.com/abstract=4489233

ABSTRACT

The surfgrass *Phyllospadix scouleri* constitutes highly productive meadows along the Pacific coast of North America – a region that has been increasingly affected by severe marine heatwaves (MHWs) in recent years. Our study assessed the effects of consecutive MHWs simulated in mesocosms on critical ecophysiological descriptors of *P. scouleri*. Generally, our results revealed a progressive deterioration of the plant overall physiological status. Surprisingly, photosynthetic parameters only indicated physiological stress once the first heat exposure ceased (i.e., recovery period). Warming induced elevated oxidative damage and a decline in nitrate uptake rates. By contrast, non-structural carbohydrates and relative growth rates remained unaffected. Our results highlight the importance of including recovery periods in this sort of experiments, as they reveal delayed stress responses. Further, the accumulative detrimental effects due to the exposure to consecutive intense MHWs indicate that these events can compromise the vitality of surfgrasses and the ecosystem services provided by their meadows.

Keywords: marine heatwave, consecutive, recovery, ecophysiology, seagrass, climate change

Abbreviations: MHWs: Marine heatwaves, Net-P_{max}: Net maximum photosynthetic rate, Gross-P_{max}: Gross maximum photosynthetic rate, R: dark respiration, α: Photosynthetic efficiency, E_c: Compensation Irradiance, E_k: Saturating irradiance, F_v/F_m: Maximum quantum yield, ETR = Electron transport rate, Φ_{PSII}: Effective quantum yield, NPQ: Non-photochemical quenching, Chl*a*: Chlorophyll *a* content, Chl*b*: Chlorophyll *b* content, $\delta^{15}N$: Nitrogen isotopic signal ($^{15}N/^{14}N$).

Preprint not peer reviewed

This preprint research paper has not been peer reviewed. Electronic copy available at: https://ssrn.com/abstract=4489233

1. Introduction

Marine ecosystems are being threatened globally by more frequent and intense marine heatwaves (MHWs) (Fox-Kemper et al., 2021). Seagrasses are ranked as one of the most valuable marine biological systems worldwide and have been severely impacted by ocean warming and MHWs globally (de los Santos et al., 2020; Strydom et al., 2020; Garrabou et al., 2022). MHWs have the potential to negatively impact seagrass vitality and community structure and cause significant die-off events, thus threatening the ecological services and goods they provide (Serrano et al., 2021; Unsworth et al., 2022).

The interaction between seagrasses and rising temperatures has received considerable attention in the last decade (Koch et al., 2013; Duarte et al., 2018; Nguyen et al., 2021). The tolerance of seagrasses to warming depends mainly on complex interactions among their stress responses (i.e., phenotypic plasticity) at different organizational levels (e.g., molecular, physiological, morphological, and community) (Deguette et al., 2022; Pazzaglia et al., 2021). The thermal tolerance of seagrasses varies depending on the thermal evolutionary history of the species, with tropical species generally being more tolerant than temperate species (Hyndes et al., 2016). On the other hand, ecotypes and genotypes of a species may also exhibit different capacities for thermal adaptation and acclimation depending on the specific temperature regime they naturally experience in their native environment (e.g., Marín-Guirao et al., 2016, 2018; Nguyen et al., 2021b; Stipcich et al., 2022). Symptoms of metabolic stress that usually occur when warming exceeds the metabolic tolerance of plants are a decrease in photosynthetic performance, depletion of internal carbon stocks, and reduced plant growth (e.g., Collier et al., 2011; Collier & Waycott, 2014; Marín-Guirao et al., 2018).

Preprint not peer reviewed

This preprint research paper has not been peer reviewed. Electronic copy available at: https://ssrn.com/abstract=4489233

The effects of MHWs on seagrasses have usually been studied in controlled experiments based on the exposure to one warming event (e.g., Costa et al., 2021; Nguyen et al., 2021a; Deguette et al., 2022; Vivanco-Bercovich et al., 2022). However, these experimental approaches overlook that MHWs can repeatedly impact seagrass meadows, as the frequency of these events is rising globally (Laufkötter et al., 2020; Fox-Kemper et al., 2021). The effects of consecutive warming events have only been addressed in a few recent manipulative studies (e.g., DuBois et al., 2020; Nguyen et al., 2020; Saha et al., 2020; Pazzaglia et al., 2022a). Pre-exposure of seagrasses to mild temperature stress could act as `eu-stress´ (*sensu* Lichtenthaler, 1998) promoting physiological strengthening and thermo-tolerance to successive MHWs (i.e., stress memory) as documented for *Posidonia australis, Posidonia oceanica* and *Zostera muelleri* (Nguyen et al., 2020; Pazzaglia et al., 2022a). Conversely, three consecutive MHWs with increasing intensity resulted in a cumulative growth weakening in *Zostera marina* (Saha et al., 2020). The intensity of the first warming event could possibly determine the magnitude and direction of seagrass responses to subsequent MHWs. Hence, assessing the effects of consecutive and intense MHWs can help to better understand the resilience of seagrasses to thermal stress associated with ongoing climate change.

Surfgrasses (*Phyllospadix scouleri* Hooker and *Phyllospadix torreyi* S.Watson) are the only seagrasses able to colonize wave-exposed rocky substrates (Cooper & McRoy, 1988). Surfgrasses form extensive and highly productive meadows along the Pacific coast of North America, from Alaska (USA) to Baja California Sur in Mexico (Den Hartog, 1970; Ramírez-García et al., 2002; Garcia-Pantoja et al., 2020), regulating important coastal physico-chemical and biological processes, and providing food and shelter for several marine

Preprint not peer reviewed

This preprint research paper has not been peer reviewed. Electronic copy available at: https://ssrn.com/abstract=4489233

organisms (Shelton, 2010; Moulton & Hacker, 2011). The Baja California Peninsula Pacific coastline, under the southernmost influence of the California Current System (Durazo, 2015), is susceptible to drastic and unpredictable ecological and economic impacts due to climate change (Xiu et al., 2018; Sunday et al., 2022). In this region, episodic thermal anomalies such as ENSO and MHWs (e.g., "the Blob" in 2014-2016, Sen Gupta et al., 2020) have caused deleterious effects in kelp forest (Arafeh-Dalmau et al., 2019; Michaud et al., 2022), but incredibly the effects on surfgrasses have been poorly documented. For instance, Pedraza-Venegas (2019) reported the disappearance of intertidal *P. scouleri* meadows near its southern distribution limit in Baja California Sur after the incidence of strong MHWs and hurricanes. In contrast, Menge et al. (2020) reported increased growth rates with increasing intertidal water temperature on intertidal *P. scouleri* populations along the Oregon and California (USA) coastline from 2008-2013.

Only a few studies (Drysdale & Barbour, 1975; Drew 1979; Ruiz-Montoya et al., 2021; Vivanco-Bercovich et al., 2022) have assessed the physiological responses of *P. torreyi* under experimental warming conditions, while thermal metabolic tolerance of *P. scouleri* remains largely unknown to date. Furthermore, most studies on surfgrasses have been conducted using intertidal plants, which may respond to warming differently from subtidal plants due to the specific regimes of environmental variables (including temperature) they naturally experience. While intertidal *Phyllospadix* plants can be exposed to a temperature rise from 22 to ~40°C within a few minutes-hours due to periodic tidal cycles (Ruiz-Montoya et al., 2021), subtidal plants are subjected to a much narrower range of daily temperature variation (e.g., usually < 3°C at the donor meadow of this study). The subtidal portions of the meadow are generally larger and denser than the intertidal portions (Garcia-Pantoja et al., 2020), and

Preprint not peer reviewed

This preprint research paper has not been peer reviewed. Electronic copy available at: https://ssrn.com/abstract=4489233

play a critical role for the intertidal plant recruitment (Williams, 1995). Understanding the capacity of subtidal surfgrasses to withstand realistic thermal disturbance regimes associated with climate change is therefore critical for anticipating the future of these vital foundation species and their related ecosystem services.

In this study, we conducted a manipulative mesocosm experiment to assess the ability of subtidal plants of *P. scouleri* to cope with a realistic regime of thermal perturbations associated with climate change. The investigation examined the effects of two consecutive MHWs on a broad set of ecophysiological descriptors (photobiology, nutrient acquisition, oxidative stress, and growth) at the end of each thermal event and its respective recovery period. With this study, we aimed to provide the first insights into the effects of MHWs on subtidal *P. scouleri.*

2. Material and methods

2.1. Plant collection, field conditions, and experimental design

Phyllospadix scouleri was collected in August 2020 in a meadow located on Todos Santos Island (Ensenada, Baja California, Mexico, 31° 48' 25.66" N, 116° 47' 46.41" O), belonging to the Pacific Islands Biosphere Reserve (Fig. 1A-C). The meadow is located in the infralittoral zone (~5 m below MHWL) of a rocky and wave-exposed shoreline, exposed to an annual seawater temperature range between 15-20ºC and episodic peaks (e.g., MHWs) reaching up to 24°C (Schlegel, 2020). Plants were detached from their substrate by slowly inserting a plastic spatula between the rock and the plant´s adhesion disc (formed by roots,

Preprint not peer reviewed

This preprint research paper has not been peer reviewed. Electronic copy available at: https://ssrn.com/abstract=4489233

rhizomes, and adhesive mucilage), while carefully pulling the clump of shoots to keep their clonal integrity as much as possible.

After collection, plants were transported in coolers (within 2 h) filled with seawater to the experimental facilities of the Instituto de Investigaciones Oceanológicas (Universidad Autónoma de Baja California). The plants were randomly allocated in a mesocosm system consisting of eight independent aquaria (60 L). Each aquarium contained 5-6 shoot clumps, which were formed by approximately 50 shoots each and were attached to one rock each to prevent them from floating. Plants were acclimated for five days at 18°C, 150-180 µmol photon m^{-2} s^{-1} with a photoperiod of 14:10 (dark: light) and a salinity of 33, according to average summer values at the donor meadow. The light was provided by LED lamps (150W), while chillers and submersible quartz heaters controlled the temperature. Submersible pumps were installed in each aquarium to allow water circulation and avoid temperature gradients. Light and temperature were monitored throughout the experiment by using submersible light/temperature sensors (Onset-HOBO MX2202), and salinity and pH were monitored using a multiparameter submersible probe (HACH HQd, YSI Professional Plus). Seawater was partially replaced (50 %) every two days with filtered (1 µm) UV-treated seawater.

After the acclimation period, conditions remained unchanged in half of the tanks (Control treatment, N = 4). In contrast, the other half were subjected to a seawater warming regime consisting of two consecutive MHWs, followed by corresponding recovery periods (MHWs treatment, N = 4). The temperature of the MHWs treatment was adjusted according to the characteristics of MHWs historically recorded in Todos Santos Island (see Fig. SM 1, Supplementary material) using the Marine Heatwave Tracker (Schlegel, 2020). The experimental thermal regime included two consecutive MHWs (HW-1 and HW-2) with their

Preprint not peer reviewed

This preprint research paper has not been peer reviewed. Electronic copy available at: https://ssrn.com/abstract=4489233

160 respective recovery periods (R-1, and R-2). For the MHWs the temperature was increased at
161 a rate of +2°C per day and maintained for five days at the maximum temperature of 24°C.
162 Thereafter temperature returned to 18°C (-2°C per day) for a 5-day recovery period. Plant
163 responses were analyzed at the end of MHWs and recovery period (Fig. 1D, E). To obtain
164 reference values for the biological status of plants in the field (Table SM 1, Supplementary
165 material), photobiological descriptors were measured immediately after plant collection, and
166 leaf tissues were frozen (-80°C) to perform further biological analysis following the methods
167 described below.

168

169 ## 2.2. Physiological traits and growth

170 For most biological variables, measurements were performed in two plants per aquarium and
171 averaged to obtain a true replicate (N = 4). P-E curves and leaf growth were determined on a
172 single shoot per aquarium, while nitrate uptake measurements were made on three shoots.
173 All measurements were conducted on the middle section of the second mature leaf to reduce
174 the variability of biological descriptors within/among leaves as possible.

175 ### *2.2.1. Photosynthesis and Respiration (P vs. E curves)*

176 Photosynthesis (P) and respiration (R) rates were determined in leaf segments using
177 respirometers composed of 200 mL borosilicate jacketed chambers connected to a
178 temperature-controlled circulating bath, and surrounded by four LED light sources (Fig. SM
179 2). Oxygen evolution was measured by optodes (DP-PSt3, PreSens, Germany), connected to
180 a fiber-optic oxygen meter (OXY4 SMA, PreSens, Germany) and controlled by software
181 (Measurement Studio 2, PreSens, Germany). A leaf biomass/seawater volume ratio of about
182 0.03-0.05 g DW L^{-1} was used to ensure accurate measurements of photosynthetic rates. Leaf

Preprint not peer reviewed

This preprint research paper has not been peer reviewed. Electronic copy available at: https://ssrn.com/abstract=4489233

segments were initially incubated in darkness for 10 min to determine R and then exposed to nine increasing PAR irradiance steps up to 806 µmol photon m^{-2} s^{-1}, each lasting 5 min. Light intensities within the chamber were previously calibrated using a spherical (4π) quantum sensor (Biospherical Instruments; California, USA). The maximum net photosynthetic rate (Net-P_{max}; µmol O_2 g^{-1} DW h^{-1}) was determined by averaging the maximum values above the saturating irradiance (E_k = net-P_{max}/ α; µmol photon m^{-2} s^{-1}). Maximum gross photosynthesis (Gross-P_{max}; µmol O_2 g^{-1} DW h^{-1}) was calculated as the sum of Net-P_{max} and R. Photosynthetic efficiency (α) was calculated as the slope of the regression line fitted to the initial linear part of the P *vs*. E curve. The compensation irradiance (E_c; µmol photon m^{-2} s^{-1}) was determined as the intercept of the initial linear part of the curve on the X-axis.

2.2.2. Daily Productivity

A proxy of daily net-productivity (DP, µmol O_2 g^{-1} DW day^{-1}) was calculated, considering the average light availability within the plant´s canopy in the aquaria (~100 µmol photon m^{-2} s^{-1}) and the selected photoperiod (14:10, dark: light). DP was calculated as [(net-P_{100} x 10) - (R x 14)], where net-P_{100} is the net photosynthesis corresponding to the irradiance at 100 µmol photon m^{-2} s^{-1} of P-E curves.

2.2.3. Chlorophyll a fluorescence and leaf absorptance

The chlorophyll *a* fluorescence emission of PSII was measured using a portable Diving-PAM fluorometer (Walz, Germany). The leaf surface was carefully cleaned off epiphytes and held in the fluorometer DCL-8 leaf-clip holder to ensure a constant distance between the tissue and the fiber optic of the fluorometer. Maximum quantum yield (F_v/F_m), and minimum and maximum fluorescences (F_0, F_m) were obtained from plants kept in darkness overnight. The exact position of the leaf where the measurements were taken was marked with small clips.

Preprint not peer reviewed

This preprint research paper has not been peer reviewed. Electronic copy available at: https://ssrn.com/abstract=4489233

206 Values of effective quantum yield (Φ_{PSII}), F_0', and F_m' were obtained at midday from light-
207 acclimated plants and illuminated with the actinic light (175 µmol photon m^{-2} s^{-1}) of the
208 fluorometer. The intensity of the actinic light was adjusted to the light intensity provided by
209 aquaria lamps. According to previous trials of induction curves, an illumination period of 90
210 seconds was selected to ensure a steady photosynthetic state at this irradiance. Non-
211 photochemical quenching, NPQ, was calculated as $(F_m-F_{m'})/F_{m'}$. Absolute ETR was
212 calculated as $ETR = \Phi_{PSII} \cdot 175 \cdot A \cdot 0.5$, where A is the leaf absorptance (see below), 175
213 is the actinic-light intensity, and 0.5 is a constant assuming that half of the incident photons
214 is absorbed by the PSII (Beer et al., 2014). For measuring leaf absorptance, the miniature
215 quantum sensor of the fluorometer was attached to the fluorometer clip holder. A leaf
216 (pigmented and bleached) was positioned over the sensor. The quantum sensor recorded the
217 actinic light emitted by the fiber optic of the fluorometer attached to the clip holder. Leaf
218 absorptance (A) was estimated as A = 1 - (LT / L0) - TW, where LT is the transmitted light
219 through the leaf tissue, L0 is the total incident light emitted by the fluorometer fiber optic
220 without leaf tissue, and TW is the transmitted light through a bleached leaf
221 (Vásquez-Elizondo et al. 2017).

222 *2.2.4. Pigment content*

223 Leaf pigments were extracted from 10 – 15 mg FW leaf tissue, homogenized in 100%
224 acetone, with $MgCO_3$ solution added to prevent the acidification of the extract (Dennison,
225 1990). Extracts were stored at 4°C in the dark for 24 h. After centrifugation (1000 x g, 10
226 min), absorbance was measured spectrophotometrically at 470, 646, and 663 nm, using 1 mL
227 cuvettes. The Chlorophylls *a*, *b,* and total carotenoids concentrations were calculated using
228 the equations described by Lichtenthaler & Wellburn (1983) and expressed as mg g^{-1} FW.

Preprint not peer reviewed

This preprint research paper has not been peer reviewed. Electronic copy available at: https://ssrn.com/abstract=4489233

2.2.5. Lipid peroxidation

Oxidative damage was evaluated by malondialdehyde (MDA) quantification following the thiobarbituric acid-reactive-substances (TBARS) assay, described by Hodges et al. (1999) and Correia et al. (2006). Ultrafrozen leaf tissue (0.2 g FW) was mechanically ground in 2 mL 80% ethanol, centrifuged for 10 min (3000 x g, 4°C), and the supernatant was added to a solution of trichloroacetic acid (20% TCA) and thiobarbituric acid (0.5% TBA). Blanks were prepared by adding the supernatant to a solution of 20% TCA. These two solutions were heated at 90°C for 30 min, and then centrifuged again (3000 x g) for 10 min. The supernatants were extracted, and their absorbance (440, 532, and 600 nm) was determined spectrophotometrically. Lipid peroxidation was expressed as equivalents of malonil-dialdehyde (Eq MDA; molar extinction coefficient 155 mM cm^{-1}), which were calculated using the equations in Hodges et al. (1999).

2.2.6. Total phenolic content and antioxidant capacity

Phenolic and antioxidant compounds were extracted from dried ground leaf tissue (0.02 g DW) in 1 mL 80% methanol in darkness for 24 h. The extract was then centrifuged at 10,000 rpm for 10 min. The phenolic compound content was determined according to a modification of the Folin–Ciocalteu assay using gallic acid as standard (Singleton & Rossi 1965). The methanolic extract (0.01 mL) was diluted in 1mL distilled water (dH_2O), 0.1 mL Folin–Ciocalteu reagent, and 0.3 mL dH_2O saturated with $NaCO_3$. This mixture was homogenized, heated (40°C for 3 min), and its absorbance read spectrophotometrically at 765 nm. Total phenolic content was expressed as gallic acid equivalents (mg Eq. GA g^{-1} DW). The radical scavenging activity was quantified according to Sabeena-Farvin & Jacobsen (2013); the reaction mixture was prepared with 0.1 mL of diluted extract (1:10 with 80% methanol) and

Preprint not peer reviewed

This preprint research paper has not been peer reviewed. Electronic copy available at: https://ssrn.com/abstract=4489233

1 mL of 60 µM 2,2-diphenyl-1-picrylhydrazyl (DPPH) dissolved in 90% methanol. The absorbance was measured at 517 nm 30 min after DPPH addition. The total antioxidant capacity was expressed as ascorbic acid equivalents (mg Eq. AA g^{-1} DW).

2.2.7. Nitrate uptake rate, nitrogen content, and nitrogen isotopic signal

The leaves from three shoots per aquarium were incubated for 30 min in independent plastic containers filled with 6 L of filtered (5 µm) and UV-treated seawater supplemented with ^{15}N tracer ($K^{15}NO_3$ at 99%, Cambridge Isotope Laboratories) at 20 µM. This nitrate concentration was selected according to the maximum values of this nutrient during upwelling near the collection site (Espinosa-Carreón et al., 2001). Incubations were performed in large incubators under constant temperature and irradiance, corresponding to each treatment's conditions. Magnetic stirrers constantly homogenized the tracer in the seawater. A leaf biomass/seawater volume ratio of 0.3 g FW L^{-1} was used in each incubation to avoid a decrease in nitrate concentration and thus, underestimation of N-uptake. At the end of the incubations, leaf tissues were rinsed with deionized water to remove the tracer adsorbed to their surfaces and dried at 60°C until constant weight. After that, samples were ground to a fine powder for isotope enrichment analyses. Isotopic determinations were performed at UC-Davis Stable Isotope Facility using an elemental analyzer (EA) interfaced with a continuous flow isotope ratio mass spectrometer (IRMS). Nitrate uptake rates (expressed as µmol N g^{-1} DW h^{-1}) were calculated using the equations shown in Sandoval-Gil et al. (2015). Nitrogen content and nitrogen isotopic signal, $\delta^{15}N$, were analyzed similarly in leaf tissues not exposed to the tracer.

Preprint not peer reviewed

This preprint research paper has not been peer reviewed. Electronic copy available at: https://ssrn.com/abstract=4489233

2.2.8. Non-structural carbohydrates

Total soluble non-structural carbohydrates (free sugars and starch) were determined using the colorimetric phenol-sulfuric acid method (Dubois et al., 1956), with glucose as the standard. Leaf tissues were oven-dried at 60°C until constant weight and ground to a fine powder. The powder was digested in 0.1 N HCl (60 ºC, 3 h), centrifuged (4000 x g, for 5 min), and the supernatant was mixed with 3% phenol and concentrated sulfuric acid. Absorbance was measured spectrophotometrically at 490 nm. Non-structural carbohydrate content was expressed in mg g^{-1} DW.

2.2.9. Relative leaf growth rate

At the beginning of each simulated MHW (HW-1 and HW-2) and each recovery phase (R-1 and R-2), the leaves of one shoot per aquarium were marked following the hole-punching method adapted from Zieman (1974). All marked shoots were collected at the end of each experimental period, and leaf segments below the mark (i.e., newly formed tissue) were dried and weighted for all leaves of each shoot. Shoot growth was expressed as relative to the total shoot biomass or relative leaf growth rate (RGR; mg g^{-1} DW day^{-1}).

2.3. Statistical analysis

Two-way Analysis of Variance (ANOVA) was used to test for the main and interactive effects of the factors Treatment ("Trt.", 2 levels: Control and MHWs) and "Time" ("Time", 4 levels: HW-1, R-1, HW-2, R-2) for each biological descriptor. In case of significant interaction ($P < 0.05$), Tukey HSD *post-hoc* tests were used to compare individual means between the Control group and the MHWs group at each sampling time. Data that did not meet the assumptions of normality (Shapiro-Wilk normality test, $P > 0.05$) or homogeneity of variances (Bartlett test, $P > 0.05$) were corrected with logarithmic transformations (i.e.,

Preprint not peer reviewed

This preprint research paper has not been peer reviewed. Electronic copy available at: https://ssrn.com/abstract=4489233

296 E_k, E_c, phenolic content, nitrate uptake). If the data remained heteroscedastic (R, Φ_{PSII}, NPQ,
297 lipid peroxidation, and $\delta^{15}N$), the model was adjusted with "White-corrected" covariance
298 matrices (Long & Ervin, 2000). Univariate analyses were performed using the statistical
299 software R (R CoreTeam 2020).

300 A Permutational Multivariate Analysis of Variance (PERMANOVA) was performed to test
301 if the different temperature treatments led to statistically significant changes in the biology
302 of *P. scouleri*. Analyses were based on the Euclidean distance matrix of normalized data.
303 PERMANOVA tested for the main and interactive effects of the fixed factor "Treatment"
304 ("Trt.", 2 levels: Control vs. MHWs) and the fixed factor "Time" (4 levels: HW-1, R-1, HW-
305 2, R-2). Pair-wise comparisons were performed between different Time levels for each
306 Treatment, where the P-values were corrected by Monte Carlo test and Bonferroni
307 adjustment. PERMANOVA was run with PRIMER 6 (Anderson et al., 2008).

308

309 3. Results

310 PERMANOVA Multivariate analyses indicated that the overall response of *P. scouleri* was
311 significantly different among treatments and sampling times (Table 1). Plants exposed to
312 warming (i.e., MHWs treatment) presented a significant variation of their physiology among
313 sampling times. In contrast, physiological changes in the control plants were not significant
314 (Pairwise PERMANOVA tests between sampling times). Also, significantly different
315 physiological responses between treatments were observed at the end of the experiment (i.e.,
316 R-2) (Pairwise PERMANOVA tests between treatments).

Preprint not peer reviewed

This preprint research paper has not been peer reviewed. Electronic copy available at: https://ssrn.com/abstract=4489233

In plants exposed to MHWs, maximum photosynthetic capacities (gross- and net-P_{max}; Fig. 2A, B) and E_k (Fig. 2C) progressively decreased by ~50 % from HW-1 to R-2 ($P < 0.001$, Table SM 2). No significant differences were found for the E_c (Fig. 2D), photosynthetic efficiency (α, Fig. 2E), and R (Fig. 2F) (Table SM 2).

Maximum photochemical efficiency (F_v/F_m, Fig. 3A), effective quantum yield (Φ_{PSII}, Fig. 3B) and electron transport rate (ETR, Fig. 3C) significantly decreased in plants after recovery phases (Table SM 2, $P < 0.05$), showing the highest reduction at the last recovery period (R-2), when those variables presented values 10, 36 and 31 % lower than the control, respectively. Conversely, NPQ in warmed plants nearly doubled in both recovery periods (R-1, R-2), compared to control plants (Fig. 3D, Table SM 2, $P < 0.001$).

Chl*a* and carotenoids significantly increased by 30 % and 35 % in plants exposed to the first heatwave (HW-1) with respect to the control (Fig. SM 3A, C; Table SM 2, $P < 0.05$). In contrast, Chl*a* and *b* were in lower concentration in warmed plants at the second heatwave (HW-2) (Fig. SM 3A, B, $P < 0.05$). Values of the Chl *b/a* ratio were higher in warmed plants than in the control at the first HW, but lower during the second recovery period (Fig. SM 3C, Table SM 2, $P < 0.05$.

In warmed plants, lipid peroxidation was significantly higher (Fig. 4A, Table SM 2, $P < 0.001$). The most significant differences occurred during both experimental heatwaves (an increase by 22 % in HW-1 and by 49 % in HW-2) (Fig. 4A). Conversely, phenolic content and antioxidant capacity were lower in warmed plants (Fig. 4B, C, Table SM 2). Phenolic content decreased by 22 % in R-2 and 32 % in HW-2 compared to the control (Fig. 4B), while antioxidant capacity was 10 % - 30 % lower during the entire experiment (Fig. 4C).

Preprint not peer reviewed

This preprint research paper has not been peer reviewed. Electronic copy available at: https://ssrn.com/abstract=4489233

Nitrate uptake rates were substantially reduced (Table SM 2, $P < 0.001$) in plants exposed to MHW with respect to the control in all sampling times, and the differences were more significant in HW-1 and R-2 (-80 %, Fig. 5A). There were no significant differences between treatments for leaf N-content (Fig. 5B). Values of $\delta^{15}N$ progressively increased towards the end of the experiment in warmed plants respect to control values (Fig. 5C, Table SM 2, $P < 0.01$).

The content of non-structural carbohydrates (Fig. 6A) was not different between control and MHW plants (Table SM 2). In contrast, the MHW treatment significantly affected the daily productivity (Fig. 6B, Table SM 2, $P < 0.001$). Values were lower (by 29 % – 52 %) in warmed plants compared to control, with the largest differences found for R-2 (Fig. 6B). Relative growth rate was not significantly affected by treatments (Fig. 6C).

4. Discussion

The results of this study showed that recurrent and intense MHWs (+6°C) can induce a progressive ecophysiological debilitation of subtidal *P. scouleri* plants, which was especially evident once exposures to warming ceased (i.e., recovery phases) (Fig. 7). Particularly, MHWs promoted a substantial reduction of nitrogen uptake capabilities and led to oxidative damage and exhaustion of antioxidant responses. Adverse effects on plant photosynthesis were most evident during the recovery phases, indicating a time lag in the response of *P. scouleri* to increased temperature. These lag effects, which appear to be more intense during the second heat wave, decreased seagrass daily productivity. Overall, our results indicate that repeated exposure to MHWs can overcome the thermal tolerance and resilience of the surfgrass *P. scouleri*.

Preprint not peer reviewed

This preprint research paper has not been peer reviewed. Electronic copy available at: https://ssrn.com/abstract=4489233

Phyllospadix scouleri did not show signs of physiological stress at the photosynthetic level (i.e, P_{max}, E_k, E_c, F_v/F_m, Φ_{PSII}, ETR) during the first experimental warming (i.e., HW-1, Figs. 2, 3). Similarly, Vivanco-Bercovich et al. (2022) found that maximum photosynthetic capacities and photochemical efficiency can be maintained (or even enhanced) in the surfgrass *Phyllospadix torreyi* exposed to warming simulating a MHW. Within metabolic tolerance ranges, warming can stimulate photosynthesis by enhancing the enzymatic activity and facilitating the mobility of proteins within the thylakoid membranes (Masini & Manning, 1997; Beca-Carretero et al., 2018). However, in our study, *P. scouleri* subjected to consecutive MHWs exhibited delayed and progressive declines in its photosynthetic performance. Values of net-P_{max}, ETR, F_v/F_m and Φ_{PSII} mostly dropped in plants recovering from each experimental warming event, reaching minimum values in the second recovery phase, R-2. For instance, the F_v/F_m dropped from ~0.76 in HW-1 to ~0.65 in R-2, probably reflecting the accumulation of heat-induced damage on the PSII. Beyond metabolic thermal resistance, heat stress can directly affect the structure and functionality of the PSII by increasing the fluidity of thylakoid membranes and dislodging key proteins (Mathur et al., 2014). Heat can induce the dissociation of its manganese cluster oxygen-evolving complex of PSII (Mathur et al., 2014), hamper reaction centers functionality due to the thermolability of the D1 protein (Rokka et al., 2000), and reduce the quantum efficiency by separating reaction centers from the light-harvesting complexes, thus blocking energy transfer and decelerating electron transport carriers (Briantais et al., 1996; Pospíšil & Tyystjärvi, 1999). These and other potential heat-induced alterations along downstream photo-assimilation processes (e.g., carbon fixation/assimilation) likely contributed to the diminished photosynthetic capacity observed, as reported for other seagrasses (e.g., Marín-Guirao et al., 2016; Costa et al., 2021; Deguette et al., 2022). On the contrary, MHW had less impact on

Preprint not peer reviewed

This preprint research paper has not been peer reviewed. Electronic copy available at: https://ssrn.com/abstract=4489233

pigments concentrations (Chl*a* and Chl*b*, Fig. SM 3), and therefore, the light-harvesting capacity did not apparently contribute to the diminished photosynthesis.

Overall, the lowered photosynthetic capacities in plants repeatedly exposed to warming indicate a progressive deterioration of the photosynthetic apparatus. Interestingly, the photosynthetic stress was mainly manifested during the recovery periods (Fig. 7). Similar delayed thermal stress responses have been reported for other seagrass species such as *Cymodocea nodosa* and *Zostera marina* (Franssen et al., 2011; Winters et al., 2011; Jueterbock et al., 2020; Deguette et al., 2022), likely resulting from the complex interactions among photoprotection mechanisms, metabolic compensation strategies, and photosystem repair cycles (Allakhverdiev et al., 2008). Supporting this notion, the photoprotective mechanism known as non-photochemical quenching (NPQ) was uniquely activated in *P. scouleri* plants that had recovered from warming. NPQ is a mechanism through which energy is dissipated as heat through the xanthophylls cycle. Its activation post-heat stress conditions has been documented in *P. torreyi* in the intertidal zone (Ruiz-Montoya et al., 2021), as well as in other seagrass species (Chartrand et al., 2018; Ontoria et al., 2019).

The photosynthetic and photoprotective responses of *P. scouleri* were consistent with oxidative stress responses (Fig. 4). Oxidative damage related to the peroxidation of membrane phospholipids by reactive oxygen species (ROS) increased in plants at HW-1 and HW-2. Similar oxidative damage was recently reported for intertidal *P. torreyi* plants facing extreme warming and desiccation during low tide (Ruiz-Montoya et al., 2021). Surpassing antioxidant responses, ROS accumulation can damage different cellular components (e.g., proteins, chloroplast membranes, DNA), and inhibit the *de novo* synthesis of D1 protein, leading to cellular death (Apel & Hirt, 2004; Sharma et al., 2012). Our results showed that

Preprint not peer reviewed

This preprint research paper has not been peer reviewed. Electronic copy available at: https://ssrn.com/abstract=4489233

plants exposed to MHWs exhibited reduced total phenolic content and antioxidant capacities, indicating a potential decrease in their antioxidant defense mechanisms and ROS scavenging activity.

Nitrate uptake rate was another physiological process strongly affected by MHWs in *P. scouleri* (Fig. 5A). The incorporation and assimilation of nitrate include highly energy-demanding reactions, even competing with other metabolic processes for photosynthate C-skeletons and metabolic energy (Touchette & Burkeholder, 2000). The diminished photosynthetic capabilities can thus restrict the potential for nitrate uptake in *P. scouleri*. This condition limits the utilization of this primary source of N fueled by upwellings in this region (Sandoval-Gil et al., 2019), as documented for other marine macrophytes affected by MHWs (Giant kelp, Sánchez-Barredo et al., 2020). Other works have reported the downregulation of genes related to nitrate uptake and assimilation (Pazzaglia et al., 2022b), and an alteration of the activity of nitrate assimilatory enzymes (Touchette & Burkholder, 2000) in seagrasses facing metabolic imbalances related to heat stress. However, enriched nitrogen isotopic signal (i.e., higher $\delta^{15}N$), and the unaltered N-content (always higher to the N-limiting level of 1.8 % DW; Duarte 1990) found in these plants contrasted with the drop in nitrate acquisition, because the low N-uptake should led to higher discrimination against ^{15}N and reduced internal N. Likely, warming could alter other processes not assessed in our study (e.g., mobilization of N-internal resources, N-exudation rates, the acquisition of other N forms) decisive for the whole-plant nitrogen budget (e.g., Alcoverro et al., 2000; Martin et al., 2018; Alexandre et al., 2020).

The reduced photosynthetic performance of plants repeatedly exposed to warming caused a decline in their net productivity (Fig. 6B) and C-unbalance (i.e., lower photosynthetic C-

Preprint not peer reviewed

This preprint research paper has not been peer reviewed. Electronic copy available at: https://ssrn.com/abstract=4489233

gains vs. respiratory C-losses). However, leaf growth rates and non-structural carbohydrates (assumed as primary C-internal reserves) remained almost unaltered. This suggests that *P. scouleri* was able to mobilize C-reserves from other vegetative compartments (e.g., rhizomes, old leaves) to maintain plant growth, or that the experimental time in our study was not enough to detect potential growth reductions. The regulation of R (respiration) and the unaltered values of the compensation irradiance ($E_{c)}$ and photosynthetic efficiency (α) probably contributed to prolonging internal carbon storage and growth, optimizing the light utilization by young leaf tissue within the canopy (Enríquez et al., 2019). Because of leaf self-shading, light can be drastically attenuated within surfgrass canopies (up to ~90 %; Ruiz-Montoya et al., 2021), and thus sub-saturating irradiances can critically contribute to the whole-plant carbon economy (Enríquez & Pantoja-Reyes, 2005; Enríquez et al., 2019). The regulation of leaf R is critical for seagrasses facing heat stress (Marín-Guirao et al., 2016; 2018), and it could be especially relevant for those with high above/below biomass ratio, such as surfgrasses (Garcia-Pantoja et al., 2020).

An increasing frequency in MHWs, as predicted for the near future (Laufkötter et al., 2020; Fox-Kemper et al., 2021), will have detrimental effects for *P. scouleri* performance due to the accumulation of thermal-stress-induced effects. These seagrass species have been scarcely studied despite their remarkable ecological relevance along the Pacific coast of North America. During the experimental exposure to two consecutive MHWs, fast-responsive traits, such as those related to photosynthesis, nitrate acquisition, and oxidative damage, revealed a progressive deterioration of the plant´s overall physiological status. Contrastingly, variables with slower response time (e.g., internal nutrient resources, leaf growth) remained constant throughout the experiment, indicating that carbon reserves were

Preprint not peer reviewed

This preprint research paper has not been peer reviewed. Electronic copy available at: https://ssrn.com/abstract=4489233

not exhausted within our experimental timeframe. Furthermore, most of the stress effects and acclimation responses were manifested once heat stress ceased, thus demonstrating the importance of including recovery periods in future experimental approaches.

The accentuated physiological stress after the impact of the second heatwave demonstrated cumulative detrimental effects. Though we did not include a real control for assessing the performance of non-primed plants exposed to the second heatwave, our results seem to contrast with other studies, where physiological tolerance to warming was enhanced in plants pre-exposed to heat (Nguyen et al., 2020; Pazzaglia et al., 2022a). This discrepancy could also be associated with species-specific thermal tolerance ranges and different experimental conditions among studies (e.g., intensity of the first warming exposure, rate of temperature increase, duration of recovery periods). Therefore, the direction and magnitude of the effects of MHWs on seagrass performance will be defined by the frequency and intensity of the consecutive warming events. Manipulating these properties for the first warming event could help to identify temperature thresholds conditioning the stimulation of physiological "hardening" (or "stress memory") or the accumulation of stress (or metabolic weakening).

ACKNOWLEDGEMENTS

Funding: This work was supported by the CONACYT-Ciencia Básica Project (A1-S-8382) granted to J.M. Sandoval-Gil. Doctoral CONACYT (Consejo Nacional de Ciencia y Tecnología) scholarships were awarded to P. Bonet-Melià and M. Vivanco-Bercovich. N. Schubert was supported by Portuguese national funds from FCT - Foundation for Science and Technology through projects UIDB/04326/2020, UIDP/04326/2020 and LA/P/0101/2020.

Preprint not peer reviewed

This preprint research paper has not been peer reviewed. Electronic copy available at: https://ssrn.com/abstract=4489233

5. References

Alcoverro, T., Manzanera, M., Romero, J., 2000. Nutrient mass balance of the seagrass *Posidonia oceanica*: the importance of nutrient retranslocation. Mar. Ecol. Prog. Ser. 194, 13–21.

Alexandre, A., Quintã, R., Hill, P.W., Jones, D.L., Santos, R., 2020. Ocean warming increases the nitrogen demand and the uptake of organic nitrogen of the globally distributed seagrass *Zostera marina*. Funct. Ecol. 34, 1325–1335. https://doi.org/10.1111/1365-2435.13576

Allakhverdiev, S.I., Kreslavski, V.D., Klimov, V.V., Los, D.A., Carpentier, R., Mohanty, P., 2008. Heat stress: an overview of molecular responses in photosynthesis. Photosynth. Res. 98, 541. https://doi.org/10.1007/s11120-008-9331-0

Anderson, M.J., Gorley, R.N., Clarke, K.R., 2008. PERMANOVA+ for PRIMER: Guide to Software and Statistical Methods, in: PRIMER-E. Plymouth, UK.

Apel, K., Hirt, H., 2004. Reactive oxygen species: metabolism, oxidative stress, and signal transduction. Annu. Rev. Plant Biol. 55, 373–399. https://doi.org/10.1146/annurev.arplant.55.031903.141701

Arafeh-Dalmau, N., Montaño-Moctezuma, G., Martínez, J.A., Beas-Luna, R., Schoeman, D.S., Torres-Moye, G., 2019. Extreme marine heatwaves alter kelp forest community near its equatorward distribution limit. Front. Mar. Sci. 6, 499. https://doi.org/10.3389/fmars.2019.00499

Preprint not peer reviewed

This preprint research paper has not been peer reviewed. Electronic copy available at: https://ssrn.com/abstract=4489233

496 Beas-Luna, R., Micheli, F., Woodson, C.B., Carr, M., Malone, D., Torre, J., Boch, C.,
497 Caselle, J.E., Edwards, M., Freiwald, J., Hamilton, S.L., Hernandez, A., Konar, B., Kroeker,
498 K.J., Lorda, J., Montaño-Moctezuma, G., Torres-Moye, G., 2020. Geographic variation in
499 responses of kelp forest communities of the California Current to recent climatic changes.
500 Glob. Change Biol. 26, 6457–6473. https://doi.org/10.1111/gcb.15273

501 Beca-Carretero, P., Olesen, B., Marbà, N., Krause-Jensen, D., 2018. Response to
502 experimental warming in northern eelgrass populations: comparison across a range of
503 temperature adaptations. Mar. Ecol. Prog. Ser. 589, 59–72.
504 https://doi.org/10.3354/meps12439

505 Beer, S., Björk, M., Beardall, J., 2014. Photosynthesis in the marine environment. John Wiley
506 & Sons.

507 Briantais, J.-M., Dacosta, J., Goulas, Y., Ducruet, J.-M., Moya, I., 1996. Heat stress induces
508 in leaves an increase of the minimum level of chlorophyll fluorescence, F_o: A time-resolved
509 analysis. Photosynth. Res. 48, 189–196. https://doi.org/10.1007/BF00041008

510 Chartrand, K.M., Szabó, M., Sinutok, S., Rasheed, M.A., Ralph, P.J., 2018. Living at the
511 margins – The response of deep-water seagrasses to light and temperature renders them
512 susceptible to acute impacts. Mar. Environ. Res. 136, 126–138.
513 https://doi.org/10.1016/j.marenvres.2018.02.006

514 Collier, C.J., Uthicke, S., Waycott, M., 2011. Thermal tolerance of two seagrass species at
515 contrasting light levels: Implications for future distribution in the Great Barrier Reef. Limnol.
516 Oceanogr. 56, 2200–2210.

Preprint not peer reviewed

This preprint research paper has not been peer reviewed. Electronic copy available at: https://ssrn.com/abstract=4489233

517 Collier, C.J., Waycott, M., 2014. Temperature extremes reduce seagrass growth and induce
518 mortality. Mar. Pollut. Bull. 83, 483–490. https://doi.org/10.1016/j.marpolbul.2014.03.050

519 Cooper, L.W., McRoy, C.P., 1988. Anatomical adaptations to rocky substrates and surf
520 exposure by the seagrass genus *Phyllospadix*. Aquat. Bot. 32, 365–381.
521 https://doi.org/10.1016/0304-3770(88)90108-8

522 Correia, M.J., Osório, M.L., Osório, J., Barrote, I., Martins, M., David, M.M., 2006.
523 Influence of transient shade periods on the effects of drought on photosynthesis, carbohydrate
524 accumulation and lipid peroxidation in sunflower leaves. Environ. Exp. Bot. 58, 75–84.
525 https://doi.org/10.1016/j.envexpbot.2005.06.015

526 Costa, M.M., Silva, J., Barrote, I., Santos, R., 2021. Heatwave effects on the photosynthesis
527 and antioxidant activity of the seagrass *Cymodocea nodosa* under contrasting light regimes.
528 Oceans 2, 448–460. https://doi.org/10.3390/oceans2030025

529 de los Santos, C.B., Scott, A., Arias-Ortiz, A., Jones, B., Kennedy, H., Mazarrasa, I.,
530 McKenzie, L., Nordlund, L.M., de la Torre-Castro, M. de la T., Unsworth, R.K.F., Ambo-
531 Rappe, R., 2020. Seagrass ecosystem services: assessment and scale of benefits. Blue Value
532 Seagrasses Environ. People 19–21.

533 Deguette, A., Barrote, I., Silva, J., 2022. Physiological and morphological effects of a marine
534 heatwave on the seagrass *Cymodocea nodosa*. Sci. Rep. 12, 7950.
535 https://doi.org/10.1038/s41598-022-12102-x

536 Delgadillo-Hinojosa, F., Félix-Bermúdez, A., Torres-Delgado, E.V., Durazo, R., Camacho-
537 Ibar, V., Mejía, A., Ruiz, M.C., Linacre, L., 2020. Impacts of the 2014–2015 warm-water
538 anomalies on nutrients, *chlorophyll-a* and hydrographic conditions in the coastal zone of

Preprint not peer reviewed

This preprint research paper has not been peer reviewed. Electronic copy available at: https://ssrn.com/abstract=4489233

539 Northern Baja California. J. Geophys. Res. Oceans 125, e2020JC016473.
540 https://doi.org/10.1029/2020JC016473

541 Den Hartog, C., 1970. The sea-grasses of the world. N.-Holl. Amst.

542 Dennison, W., 1990. Chlorophyll content, in: Seagrass Research Methods. Phillips, R.C.;
543 McRoy, C.P., Paris (France) UNESCO.

544 Drew, E.A., 1979. Physiological aspects of primary production in seagrasses. Aquat. Bot. 7,
545 139–150. https://doi.org/10.1016/0304-3770(79)90018-4

546 Drysdale, F.R., Barbour, M.G., 1975. Response of the marine angiosperm *Phyllospadix*
547 *torreyi* to certain environmental variables: A preliminary study. Aquat. Bot. 1, 97–106.
548 https://doi.org/10.1016/0304-3770(75)90015-7

549 Duarte, B., Martins, I., Rosa, R., Matos, A.R., Roleda, M.Y., Reusch, T.B.H., Engelen, A.H.,
550 Serrão, E.A., Pearson, G.A., Marques, J.C., Caçador, I., Duarte, C.M., Jueterbock, A., 2018.
551 Climate change impacts on seagrass meadows and macroalgal forests: an integrative
552 perspective on acclimation and adaptation potential. Front. Mar. Sci. 5, 190.
553 https://doi.org/10.3389/fmars.2018.00190

554 DuBois, K., Williams, S.L., Stachowicz, J.J., 2020. Previous exposure mediates the response
555 of eelgrass to future warming via clonal transgenerational plasticity. Ecology 101.
556 https://doi.org/10.1002/ecy.3169

557 Dubois, M., Gilles, K.A., Hamilton, J.K., Rebers, P.A., Smith, F., 1956. Colorimetric method
558 for determination of sugars and related substances. Anal. Chem. 28, 350–356.

Preprint not peer reviewed

This preprint research paper has not been peer reviewed. Electronic copy available at: https://ssrn.com/abstract=4489233

559 Durazo, R., 2015. Seasonality of the transitional region of the California Current System off
560 Baja California. J. Geophys. Res. Oceans 120, 1173–1196.
561 https://doi.org/10.1002/2014JC010405

562 Enríquez, S., Borowitzka, M.A., 2010. The use of the fluorescence signal in studies of
563 seagrasses and macroalgae, in: *Chlorophyll a* Fluorescence in Aquatic Sciences: Methods
564 and Applications. Springer, pp. 187–208.

565 Enríquez, S., Olivé, I., Cayabyab, N., Hedley, J.D., 2019. Structural complexity governs
566 seagrass acclimatization to depth with relevant consequences for meadow production,
567 macrophyte diversity and habitat carbon storage capacity. Sci. Rep. 9, 14657.
568 https://doi.org/10.1038/s41598-019-51248-z

569 Enríquez, S., Pantoja-Reyes, N.I., 2005. Form-function analysis of the effect of canopy
570 morphology on leaf self-shading in the seagrass *Thalassia testudinum*. Oecologia 145, 234–
571 242. https://doi.org/10.1007/s00442-005-0111-7

572 Espinosa-Carreón, T.L., Gaxiola-Castro, G., Robles-Pacheco, J.M., Nájera-Martínez, S.,
573 2001. Temperature, salinity, nutrients and chlorophyll a in coastal waters of the Southern
574 California Bight. Cienc. Mar. 27, 397–422. https://doi.org/10.7773/cm.v27i3.490

575 Evans, R.D., 2001. Physiological mechanisms influencing plant nitrogen isotope
576 composition. Trends Plant Sci. 6, 121–126. https://doi.org/10.1016/S1360-1385(01)01889-1

577 Fox-Kemper, B., 2021. Ocean, Cryosphere and Sea Level Change (Ch. 9 of Climate Change
578 2021: The Physical Science Basis). Contrib. Work. Group Sixth Assess. Rep. Intergov. Panel
579 Clim. Change.

Preprint not peer reviewed

This preprint research paper has not been peer reviewed. Electronic copy available at: https://ssrn.com/abstract=4489233

580 Franssen, S.U., Gu, J., Bergmann, N., Winters, G., Klostermeier, U.C., Rosenstiel, P.,
581 Bornberg-Bauer, E., Reusch, T.B.H., 2011. Transcriptomic resilience to global warming in
582 the seagrass *Zostera marina*, a marine foundation species. Proc. Natl. Acad. Sci. 108, 19276–
583 19281. https://doi.org/10.1073/pnas.1107680108

584 Friedland, N., Negi, S., Vinogradova-Shah, T., Wu, G., Ma, L., Flynn, S., Kumssa, T., Lee,
585 C.-H., Sayre, R.T., 2019. Fine-tuning the photosynthetic light harvesting apparatus for
586 improved photosynthetic efficiency and biomass yield. Sci. Rep. 9, 13028.
587 https://doi.org/10.1038/s41598-019-49545-8

588 García-Pantoja, J.A., Ruiz-Montoya, L., Sandoval-Gil, J.M., Vivanco-Bercovich, M.V.,
589 Ferreira-Arrieta, A., Zertuche-González, J.A., Guzmán-Calderón, J.M., Norzagaray-López
590 Orión; Samperio-Ramos, G., Montaño-Moctezuma, G., Hernández-Ayón, M., 2020. Fijación
591 neta de carbono por pastos marinos (*Phyllospadix* spp.) en una isla del Pacífico Mexicano,
592 in: Estado actual del conocimiento del ciclo del carbono y sus interacciones en México:
593 Síntesis a 2020, Síntesis Nacionales. Programa Mexicano del Carbono en colaboración con
594 la Universidad Autónoma Metropolitana-Xochimilco, Texcoco, Estado de México, México,
595 p. 602.

596 Garrabou, J., Gómez-Gras, D., Medrano, A., Cerrano, C., Ponti, M., Schlegel, R.,
597 Bensoussan, N., Turicchia, E., Sini, M., Gerovasileiou, V., Teixido, N., Mirasole, A.,
598 Tamburello, L., Cebrian, E., Rilov, G., Ledoux, J.-B., Souissi, J.B., Khamassi, F., Ghanem,
599 R., Benabdi, M., Grimes, S., Ocaña, O., Bazairi, H., Hereu, B., Linares, C., Kersting, D.K.,
600 la Rovira, G., Ortega, J., Casals, D., Pagès-Escolà, M., Margarit, N., Capdevila, P., Verdura,
601 J., Ramos, A., Izquierdo, A., Barbera, C., Rubio-Portillo, E., Anton, I., López-Sendino, P.,
602 Díaz, D., Vázquez-Luis, M., Duarte, C., Marbà, N., Aspillaga, E., Espinosa, F., Grech, D.,

Preprint not peer reviewed

This preprint research paper has not been peer reviewed. Electronic copy available at: https://ssrn.com/abstract=4489233

603 Guala, I., Azzurro, E., Farina, S., Cristina Gambi, M., Chimienti, G., Montefalcone, M.,
604 Azzola, A., Mantas, T.P., Fraschetti, S., Ceccherelli, G., Kipson, S., Bakran-Petricioli, T.,
605 Petricioli, D., Jimenez, C., Katsanevakis, S., Kizilkaya, I.T., Kizilkaya, Z., Sartoretto, S.,
606 Elodie, R., Ruitton, S., Comeau, S., Gattuso, J.-P., Harmelin, J.-G., 2022. Marine heatwaves
607 drive recurrent mass mortalities in the Mediterranean Sea. Glob. Change Biol. 28, 5708–
608 5725. https://doi.org/10.1111/gcb.16301

609 Hodges, D.M., DeLong, J.M., Forney, C.F., Prange, R.K., 1999. Improving the thiobarbituric
610 acid-reactive-substances assay for estimating lipid peroxidation in plant tissues containing
611 anthocyanin and other interfering compounds. Planta 207, 604–611.
612 https://doi.org/10.1007/s004250050524

613 Hyndes, G.A., Heck, K.L., Vergés, A., Harvey, E.S., Kendrick, G.A., Lavery, P.S.,
614 McMahon, K., Orth, R.J., Pearce, A., Vanderklift, M., Wernberg, T., Whiting, S., Wilson,
615 S., 2016. Accelerating tropicalization and the transformation of temperate seagrass meadows.
616 BioScience 66, 938–948. https://doi.org/10.1093/biosci/biw111

617 Jeyapragash, D., Subhashini, P., Raja, S., Abirami, K., Thangaradjou, T., 2016. Evaluation
618 of in-vitro antioxidant activity of seagrasses: signals for potential alternate source. Free
619 Radic. Antioxid. 6, 77–89. https://doi.org/10.5530/fra.2016.1.10

620 Jueterbock, A., Boström, C., Coyer, J.A., Olsen, J.L., Kopp, M., Dhanasiri, A.K.S., Smolina,
621 I., Arnaud-Haond, S., Van de Peer, Y., Hoarau, G., 2020. The seagrass methylome is
622 associated with variation in photosynthetic performance among clonal shoots. Front. Plant
623 Sci. 11.

Preprint not peer reviewed

This preprint research paper has not been peer reviewed. Electronic copy available at: https://ssrn.com/abstract=4489233

624 Koch, M., Bowes, G., Ross, C., Zhang, X.-H., 2013. Climate change and ocean acidification
625 effects on seagrasses and marine macroalgae. Glob. Change Biol. 19, 103–132.
626 https://doi.org/10.1111/j.1365-2486.2012.02791.x

627 Laufkötter, C., Zscheischler, J., Frölicher, T.L., 2020. High-impact marine heatwaves
628 attributable to human-induced global warming. Science.
629 https://doi.org/10.1126/science.aba0690

630 Lichtenthaler, H.K., 1998. The Stress Concept in Plants: An Introduction. Ann. N. Y. Acad.
631 Sci. 851, 187–198. https://doi.org/10.1111/j.1749-6632.1998.tb08993.x

632 Lichtenthaler, H.K., Wellburn, A.R., 1983. Determinations of total carotenoids and
633 *chlorophylls a* and *b* of leaf extracts in different solvents. Biochem. Soc. Trans. 11, 591–592.
634 https://doi.org/10.1042/bst0110591

635 Marín-Guirao, L., Bernardeau-Esteller, J., García-Muñoz, R., Ramos, A., Ontoria, Y.,
636 Romero, J., Pérez, M., Ruiz, J.M., Procaccini, G., 2018. Carbon economy of Mediterranean
637 seagrasses in response to thermal stress. Mar. Pollut. Bull. 135, 617–629.
638 https://doi.org/10.1016/j.marpolbul.2018.07.050

639 Marín-Guirao, L., Ruiz, J.M., Dattolo, E., Garcia-Munoz, R., Procaccini, G., 2016.
640 Physiological and molecular evidence of differential short-term heat tolerance in
641 Mediterranean seagrasses. Sci. Rep. 6, 28615. https://doi.org/10.1038/srep28615

642 Martin, B.C., Statton, J., Siebers, A.R., Grierson, P.F., Ryan, M.H., Kendrick, G.A., 2018.
643 Colonizing tropical seagrasses increase root exudation under fluctuating and continuous low
644 light. Limnol. Oceanogr. 63, S381–S391. https://doi.org/10.1002/lno.10746

Preprint not peer reviewed

This preprint research paper has not been peer reviewed. Electronic copy available at: https://ssrn.com/abstract=4489233

645 Masini, R.J., Manning, C.R., 1997. The photosynthetic responses to irradiance and
646 temperature of four meadow-forming seagrasses. Aquat. Bot. 58, 21–36.
647 https://doi.org/10.1016/S0304-3770(97)00008-9

648 Mathur, S., Agrawal, D., Jajoo, A., 2014. Photosynthesis: Response to high temperature
649 stress. J. Photochem. Photobiol. B, Stress and Photosynthesis 137, 116–126.
650 https://doi.org/10.1016/j.jphotobiol.2014.01.010

651 Menge, B.A., Close, S.L., Hacker, S.D., Nielsen, K.J., Chan, F., 2020. Biogeography of
652 macrophyte productivity: Effects of oceanic and climatic regimes across spatiotemporal
653 scales. Limnol. Oceanogr. lno.11635. https://doi.org/10.1002/lno.11635

654 Michaud, K.M., Reed, D.C., Miller, R.J., 2022. The Blob marine heatwave transforms
655 California kelp forest ecosystems. Commun. Biol. 5, 1–8. https://doi.org/10.1038/s42003-
656 022-04107-z

657 Moulton, O.M., Hacker, S.D., 2011. Congeneric variation in surfgrasses and ocean
658 conditions influence macroinvertebrate community structure. Mar. Ecol. Prog. Ser. 433, 53–
659 63. https://doi.org/10.3354/meps09180

660 Nguyen, H.M., Bulleri, F., Marín-Guirao, L., Pernice, M., Procaccini, G., 2021a. Photo-
661 physiology and morphology reveal divergent warming responses in northern and southern
662 hemisphere seagrasses. Mar. Biol. 168, 129. https://doi.org/10.1007/s00227-021-03940-w

663 Nguyen, H.M., Kim, M., Ralph, P.J., Marín-Guirao, L., Pernice, M., Procaccini, G., 2020.
664 Stress memory in seagrasses: first insight into the effects of thermal priming and the role of
665 epigenetic modifications. Front. Plant Sci. 11, 494. https://doi.org/10.3389/fpls.2020.00494

Preprint not peer reviewed

This preprint research paper has not been peer reviewed. Electronic copy available at: https://ssrn.com/abstract=4489233

Nguyen, H.M., Ralph, P.J., Marín-Guirao, L., Pernice, M., Procaccini, G., 2021b. Seagrasses in an era of ocean warming: a review. Biol. Rev. 96, 2009–2030. https://doi.org/10.1111/brv.12736

Ontoria, Y., Cuesta-Gracia, A., Ruiz, J.M., Romero, J., Pérez, M., 2019. The negative effects of short-term extreme thermal events on the seagrass *Posidonia oceanica* are exacerbated by ammonium additions. PLOS ONE 14, e0222798. https://doi.org/10.1371/journal.pone.0222798

Pazzaglia, J., Badalamenti, F., Bernardeau-Esteller, J., Ruiz, J.M., Giacalone, V.M., Procaccini, G., Marín-Guirao, L., 2022a. Thermo-priming increases heat-stress tolerance in seedlings of the Mediterranean seagrass *P. oceanica*. Mar. Pollut. Bull. 174, 113164. https://doi.org/10.1016/j.marpolbul.2021.113164

Pazzaglia, J., Reusch, T.B.H., Terlizzi, A., Marín-Guirao, L., Procaccini, G., 2021. Phenotypic plasticity under rapid global changes: The intrinsic force for future seagrasses survival. Evol. Appl. 14, 1181–1201. https://doi.org/10.1111/eva.13212

Pazzaglia, J., Santillán-Sarmiento, A., Ruocco, M., Dattolo, E., Ambrosino, L., Marín-Guirao, L., Procaccini, G., 2022b. Local environment modulates whole-transcriptome expression in the seagrass *Posidonia oceanica* under warming and nutrients excess. Environ. Pollut. 303, 119077. https://doi.org/10.1016/j.envpol.2022.119077

Pedraza-Venegas, KV., 2019. Distribución espacio-temporal y efecto de la temperatura en praderas de *Phyllospadix scouleri* en tres localidades de B.C.S. Universidad Autónoma de Baja California Sur. Tesis de Doctorado. Universidad Autónoma de Baja California Sur.

Preprint not peer reviewed

This preprint research paper has not been peer reviewed. Electronic copy available at: https://ssrn.com/abstract=4489233

687 Pospíšil, P., Tyystjärvi, E., 1999. Molecular mechanism of high-temperature-induced
688 inhibition of acceptor side of Photosystem II. Photosynth. Res. 62, 55–66.
689 https://doi.org/10.1023/A:1006369009170

690 R Core Team, 2020. R: A language and environment for statistical computing. R Found. Stat.
691 Comput.

692 Ramírez-García, P., Terrados, J., Ramos, F., Lot, A., Ocaña, D., Duarte, C.M., 2002.
693 Distribution and nutrient limitation of surfgrass, *Phyllospadix scouleri* and *Phyllospadix*
694 *torreyi*, along the Pacific coast of Baja California (México). Aquat. Bot. 74, 121–131.
695 https://doi.org/10.1016/S0304-3770(02)00050-5

696 Rokka, A., Aro, E.-M., Herrmann, R.G., Andersson, B., Vener, A.V., 2000.
697 Dephosphorylation of photosystem II reaction center proteins in plant photosynthetic
698 membranes as an immediate response to abrupt elevation of temperature. Plant Physiol. 123,
699 1525–1536. https://doi.org/10.1104/pp.123.4.1525

700 Ruiz-Montoya, L., Sandoval-Gil, J.M., Belando-Torrentes, M.D., Vivanco-Bercovich, M.,
701 Cabello-Pasini, A., Rangel-Mendoza, L.K., Maldonado-Gutiérrez, A., Ferrerira-Arrieta, A.,
702 Guzmán-Calderón, J.M., 2021. Ecophysiological responses and self-protective canopy
703 effects of surfgrass (*Phyllospadix torreyi*) in the intertidal. Mar. Environ. Res. 172, 105501.
704 https://doi.org/10.1016/j.marenvres.2021.105501

705 Sabeena Farvin, K.H., Jacobsen, C., 2013. Phenolic compounds and antioxidant activities of
706 selected species of seaweeds from Danish coast. Food Chem. 138, 1670–1681.
707 https://doi.org/10.1016/j.foodchem.2012.10.078

Preprint not peer reviewed

This preprint research paper has not been peer reviewed. Electronic copy available at: https://ssrn.com/abstract=4489233

708 Saha, M., Barboza, F.R., Somerfield, P.J., Al-Janabi, B., Beck, M., Brakel, J., Ito, M., Pansch,
709 C., Nascimento-Schulze, J.C., Jakobsson Thor, S., Weinberger, F., Sawall, Y., 2020.
710 Response of foundation macrophytes to near-natural simulated marine heatwaves. Glob.
711 Change Biol. 26, 417–430. https://doi.org/10.1111/gcb.14801

712 Sánchez-Barredo, M., Sandoval-Gil, J.M., Zertuche-González, J.A., Ladah, L.B., Belando-
713 Torrentes, M.D., Beas-Luna, R., Cabello-Pasini, A., 2020. Effects of heat waves and light
714 deprivation on giant kelp juveniles (*Macrocystis pyrifera*, Laminariales, Phaeophyceae). J.
715 Phycol. 56, 880–894.

716 Sandoval-Gil, J.M., Barrote, I., Silva, J., Olivé, I., Costa, M.M., Ruiz, J.M., Marín-Guirao,
717 L., Sánchez-Lizaso, J.L., Santos, R., 2015. Plant-water relations of intertidal and subtidal
718 seagrasses. Mar. Ecol. 36, 1294–1310. https://doi.org/10.1111/maec.12230

719 Sandoval-Gil, J.M., del Carmen Ávila-López, M., Camacho-Ibar, V.F., Hernández-Ayón,
720 J.M., Zertuche-González, J.A., Cabello-Pasini, A., 2019. Regulation of nitrate uptake by the
721 seagrass *Zostera marina* during upwelling. Estuaries Coasts 42, 731–742.

722 Schlegel, R.W., 2020. Marine Heatwave Tracker. URL
723 http://www.marineheatwaves.org/tracker.html

724 Sen Gupta, A., Thomsen, M., Benthuysen, J.A., Hobday, A.J., Oliver, E., Alexander, L.V.,
725 Burrows, M.T., Donat, M.G., Feng, M., Holbrook, N.J., Perkins-Kirkpatrick, S., Moore, P.J.,
726 Rodrigues, R.R., Scannell, H.A., Taschetto, A.S., Ummenhofer, C.C., Wernberg, T., Smale,
727 D.A., 2020. Drivers and impacts of the most extreme marine heatwave events. Sci. Rep. 10,
728 19359. https://doi.org/10.1038/s41598-020-75445-3

Preprint not peer reviewed

This preprint research paper has not been peer reviewed. Electronic copy available at: https://ssrn.com/abstract=4489233

729 Serrano, O., Arias-Ortiz, A., Duarte, C.M., Kendrick, G.A., Lavery, P.S., 2021. Impact of
730 marine heatwaves on seagrass ecosystems, in: Ecosystem Collapse and Climate Change.
731 Springer, pp. 345–364.

732 Sharma, P., Jha, A.B., Dubey, R.S., Pessarakli, M., 2012. Reactive oxygen species, oxidative
733 damage, and antioxidative defense mechanism in plants under stressful conditions. J. Bot.
734 2012, e217037. https://doi.org/10.1155/2012/217037

735 Shelton, A.O., 2010. Temperature and community consequences of the loss of foundation
736 species: Surfgrass (*Phyllospadix* spp., Hooker) in tidepools. J. Exp. Mar. Biol. Ecol. 391, 35–
737 42. https://doi.org/10.1016/j.jembe.2010.06.003

738 Silva, J., Barrote, I., Costa, M.M., Albano, S., Santos, R., 2013. Physiological Responses of
739 *Zostera marina* and *Cymodocea nodosa* to Light-Limitation Stress. PLOS ONE 8, e81058.
740 https://doi.org/10.1371/journal.pone.0081058

741 Singleton, V.L., Rossi, J.A., 1965. Colorimetry of total phenolics with phosphomolybdic-
742 phosphotungstic acid reagents. Am. J. Enol. Vitic. 16, 144–158.

743 Stipcich, P., Marín-Guirao, L., Pansini, A., Pinna, F., Procaccini, G., Pusceddu, A., Soru, S.,
744 Ceccherelli, G., 2022. Effects of current and future summer marine heat waves on *Posidonia*
745 *oceanica*: Plant origin matters? Front. Clim. 4, 844831.
746 https://doi.org/10.3389/fclim.2022.844831

747 Strydom, S., Murray, K., Wilson, S., Huntley, B., Rule, M., Heithaus, M., Bessey, C.,
748 Kendrick, G.A., Burkholder, D., Fraser, M.W., Zdunic, K., 2020. Too hot to handle:
749 Unprecedented seagrass death driven by marine heatwave in a World Heritage Area. Glob.
750 Change Biol. 26, 3525–3538. https://doi.org/10.1111/gcb.15065

Preprint not peer reviewed

This preprint research paper has not been peer reviewed. Electronic copy available at: https://ssrn.com/abstract=4489233

751 Sunday, J.M., Howard, E., Siedlecki, S., Pilcher, D.J., Deutsch, C., MacCready, P., Newton,
752 J., Klinger, T., 2022. Biological sensitivities to high-resolution climate change projections in
753 the California current marine ecosystem. Glob. Change Biol. 28, 5726–5740.
754 https://doi.org/10.1111/gcb.16317

755 Touchette, B.W., Burkholder, J.M., 2000. Review of nitrogen and phosphorus metabolism in
756 seagrasses. J. Exp. Mar. Biol. Ecol. 250, 133–167. https://doi.org/10.1016/S0022-
757 0981(00)00195-7

758 Tutar, O., Marín-Guirao, L., Ruiz, J.M., Procaccini, G., 2017. Antioxidant response to heat
759 stress in seagrasses. A gene expression study. Mar. Environ. Res. 132, 94–102.
760 https://doi.org/10.1016/j.marenvres.2017.10.011

761 Unsworth, R.K., Cullen-Unsworth, L.C., Jones, B.L., Lilley, R.J., 2022. The planetary role
762 of seagrass conservation. Science 377, 609–613.

763 Vásquez-Elizondo, R.M., Legaria-Moreno, L., Pérez-Castro, M.Á., Krämer, W.E., Scheufen,
764 T., Iglesias-Prieto, R., Enríquez, S., 2017. Absorptance determinations on multicellular
765 tissues. Photosynth. Res. 132, 311–324. https://doi.org/10.1007/s11120-017-0395-6

766 Vivanco-Bercovich, M., Belando-Torrentes, M.D., Figueroa-Burgos, M.F., Ferreira-Arrieta,
767 A., Macías-Carranza, V., García-Pantoja, J.A., Cabello-Pasini, A., Samperio-Ramos, G.,
768 Cruz-López, R., Sandoval-Gil, J.M., 2022. Combined effects of marine heatwaves and
769 reduced light on the physiology and growth of the surfgrass *Phyllospadix torreyi* from Baja
770 California, Mexico. Aquat. Bot. 178, 103488. https://doi.org/10.1016/j.aquabot.2021.103488

Preprint not peer reviewed

This preprint research paper has not been peer reviewed. Electronic copy available at: https://ssrn.com/abstract=4489233

771 Wiencke, C., Bischof, K. (Eds.), 2012. Seaweed Biology: Novel Insights into Ecophysiology,
772 Ecology and Utilization, Ecological Studies. Springer Berlin Heidelberg, Berlin, Heidelberg.
773 https://doi.org/10.1007/978-3-642-28451-9

774 Williams, S.L., 1995. Surfgrass (*Phyllospadix torreyi*) Reproduction: Reproductive
775 Phenology, Resource Allocation, and Male Rarity. Ecology 76, 1953–1970.
776 https://doi.org/10.2307/1940726

777 Winters, G., Nelle, P., Fricke, B., Rauch, G., Reusch, T., 2011. Effects of a simulated heat
778 wave on photophysiology and gene expression of high- and low-latitude populations of
779 *Zostera marina*. Mar. Ecol. Prog. Ser. 435, 83–95. https://doi.org/10.3354/meps09213

780 Xiu, P., Chai, F., Curchitser, E.N., Castruccio, F.S., 2018. Future changes in coastal
781 upwelling ecosystems with global warming: The case of the California Current System. Sci.
782 Rep. 8, 2866. https://doi.org/10.1038/s41598-018-21247-7

783 Zieman, J.C., 1974. Methods for the study of the growth and production of turtle grass,
784 *Thalassia testudinum* König. Aquaculture 4, 139–143.

Preprint not peer reviewed

This preprint research paper has not been peer reviewed. Electronic copy available at: https://ssrn.com/abstract=4489233

6. Acknowledgments

Financial support was provided by the CONACYT-Ciencia Básica Project (A1-S-8382) granted to J.M. Sandoval-Gil. Doctoral CONACYT (Consejo Nacional de Ciencia y Tecnología) scholarships were awarded to P. Bonet-Melià and M. Vivanco-Bercovich.

7. Figure legends

Figure 1. The unaltered donor meadow of *Phyllospadix scouleri* is located at Todos Santos Island, Baja California, Mexico (A, B and C, red dot), where seawater temperature was monitored with sensors *in situ* before and during the experiment (D, black line). Seawater temperature at the mesocosm was also recorded (D, blue and red lines). The panel E shows a schematic representation of the experimental design, which consisted of one treatment (MHWs) with two consecutive warm periods (24°C) succeeded by recovery periods (18°C). A control treatment was set with constant temperature (C - 18°C). As indicated by black or red circles, biological descriptors were determined at the end of each experimental period (HW-1, R-1, HW-2, R-2).

Figure 2. Parameters derived from photosynthesis-irradiance curves determined for *P. scouleri* in response to the temperature treatments. The treatment of MHWs (red line) included two consecutive heatwaves of 24°C (red filled circles, HW-1 and HW-2) and their respective recovery periods at 18°C (red hollow circles, R-1 and R-2). A Control treatment (black line) was maintained at a constant 18°C during the entire experiment. Values are means and standard errors (N = 4). The significance of the main effects from Treatment (Trt.) and Time and their interaction term (Two-way ANOVA) is indicated at the bottom left corner

Preprint not peer reviewed

This preprint research paper has not been peer reviewed. Electronic copy available at: https://ssrn.com/abstract=4489233

of each graph. In case of significant interaction, the significance of paired comparisons (Tukey HSD *post-hoc* test) between treatments at each sampling time is indicated with asterisks on top of the relevant sampling times. *P < 0.05, **P < 0.01, ***P < 0.001, n.s.: P > 0.1 (For complete results, see Table SM 2). (A) Net-P_{max}: Net maximum photosynthetic rate, (B) Gross- P_{max}: Gross maximum photosynthetic rate, (C) E_k: Saturation Irradiance, (D) E_c: Compensation Irradiance, (E) α: Photosynthetic efficiency, (F) R: Respiration rate.

Figure 3. Chlorophyll *a* fluorescence parameters measured in *P. scouleri* in response to two temperature treatments (MHWs in red, Control in black) along four sampling times (HW-1, R-1, HW-2, R-2). The treatment of MHWs (red line) included two consecutive heatwaves of 24°C (red filled circles, HW-1 and HW-2) and their respective recovery periods at 18°C (red hollow circles, R-1 and R-2). A Control treatment (black line) was maintained at a constant 18°C during the entire experiment. Values are means and standard errors (N = 4). See further details of statistical analyses in the legend of Fig. 2. (A) F_v/F_m: Maximum photochemical efficiency, (B) Φ_{PSII}: Effective photochemical efficiency, (C) ETR: Electron transport rate, (D) NPQ: Non-photochemical quenching.

Figure 4. Lipid peroxidation (A), total phenolic content (B) and total antioxidant capacity (C) determined in *P. scouleri* leaves in response to two temperature treatments (MHWs in red, Control in black) along four sampling times (HW-1, R-1, HW-2, R-2). The treatment of MHWs (red line) included two consecutive heatwaves of 24°C (red filled circles, HW-1 and HW-2) and their respective recovery periods at 18°C (red hollow circles, R-1 and R-2). A Control treatment (black line) was maintained at a constant 18°C during the entire

Preprint not peer reviewed

This preprint research paper has not been peer reviewed. Electronic copy available at: https://ssrn.com/abstract=4489233

experiment. Values are means and standard errors (N = 4). See further details of statistical analyses in the legend of Fig. 2.

Figure 5. Nitrate uptake rate (A), nitrogen content (B) and isotopic ratio of nitrogen (C) determined in *P. scouleri* leaves in response to two temperature treatments (MHWs in red, Control in black) along four sampling times (HW-1, R-1, HW-2, R-2). The treatment of MHWs (red line) included two consecutive heatwaves of 24°C (red filled circles, HW-1 and HW-2) and their respective recovery periods at 18°C (red hollow circles, R-1 and R-2). A Control treatment (black line) was maintained at a constant 18°C during the entire experiment. Values are means and standard errors (N = 4). See further details of statistical analyses in the legend of Fig. 2.

Figure 6. Non-structural carbohydrates (A), daily productivity (B) and relative growth rate (C) determined in *P. scouleri* leaves in response to two temperature treatments (MHWs in red, Control in black) along four sampling times (HW-1, R-1, HW-2, R-2 The treatment of MHWs (red line) included two consecutive heatwaves of 24°C (red filled circles, HW-1 and HW-2) and their respective recovery periods at 18°C (red hollow circles, R-1 and R-2). A Control treatment (black line) was maintained at a constant 18°C during the entire experiment. Values are means and standard errors (N = 4). See further details of statistical analyses in the legend of Fig. 2.

Figure 7. A graphical representation that summarizes the main responses and effects observed in *P. scouleri* plants after being exposed to two consecutive heatwaves (HW-1 and HW-2) with recovery periods (R-1 and R-2). The behavior of general physiological

Preprint not peer reviewed

This preprint research paper has not been peer reviewed. Electronic copy available at: https://ssrn.com/abstract=4489233

854 processes/features (bold letters and vertical arrows) is based on the measurements of
855 representative biological descriptors (italic letters). Only biological variables that showed
856 statistically significant changes were considered (Two-way ANOVA with significant
857 interaction term and *post-hoc* Tukey-HSD test with $P < 0.05$). Gross-Pmax: Gross maximum
858 photosynthetic capacity, Net-Pmax: Net maximum photosynthetic capacity, E_k: Saturation
859 irradiance, F_v/F_m: Maximum quantum yield, Φ_{PSII}: Effective quantum yield, ETR: Electron
860 transport rate, NPQ: Non-photochemical quenching, N (% DW): Nitrogen content, NSC:
861 Non-structural carbohydrates, RGR: Relative growth rate.

Preprint not peer reviewed

This preprint research paper has not been peer reviewed. Electronic copy available at: https://ssrn.com/abstract=4489233

862 8. Figures

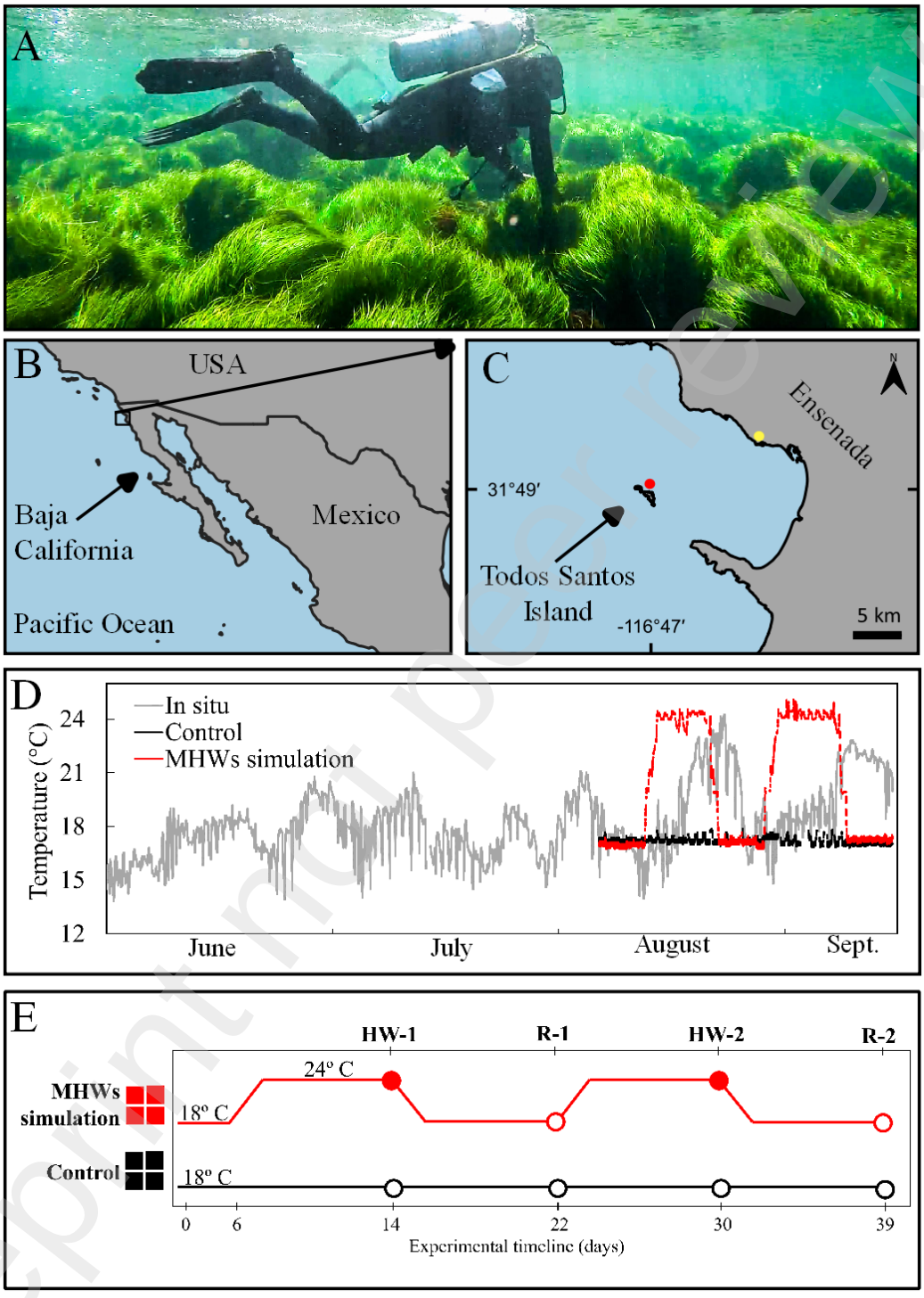

863

864 Fig. 1.

Preprint not peer reviewed

This preprint research paper has not been peer reviewed. Electronic copy available at: https://ssrn.com/abstract=4489233

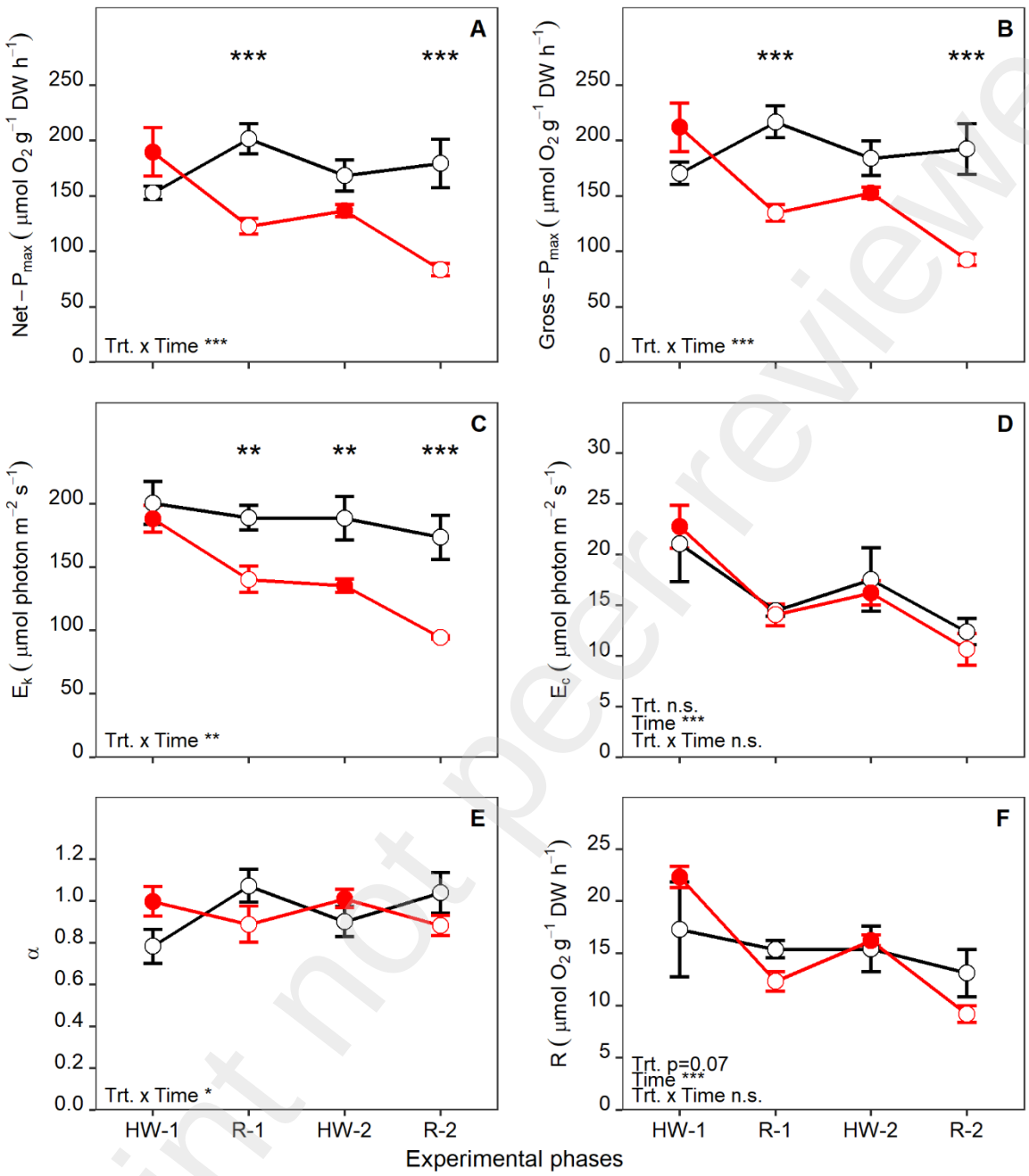

865

866 Fig. 2.

Preprint not peer reviewed

This preprint research paper has not been peer reviewed. Electronic copy available at: https://ssrn.com/abstract=4489233

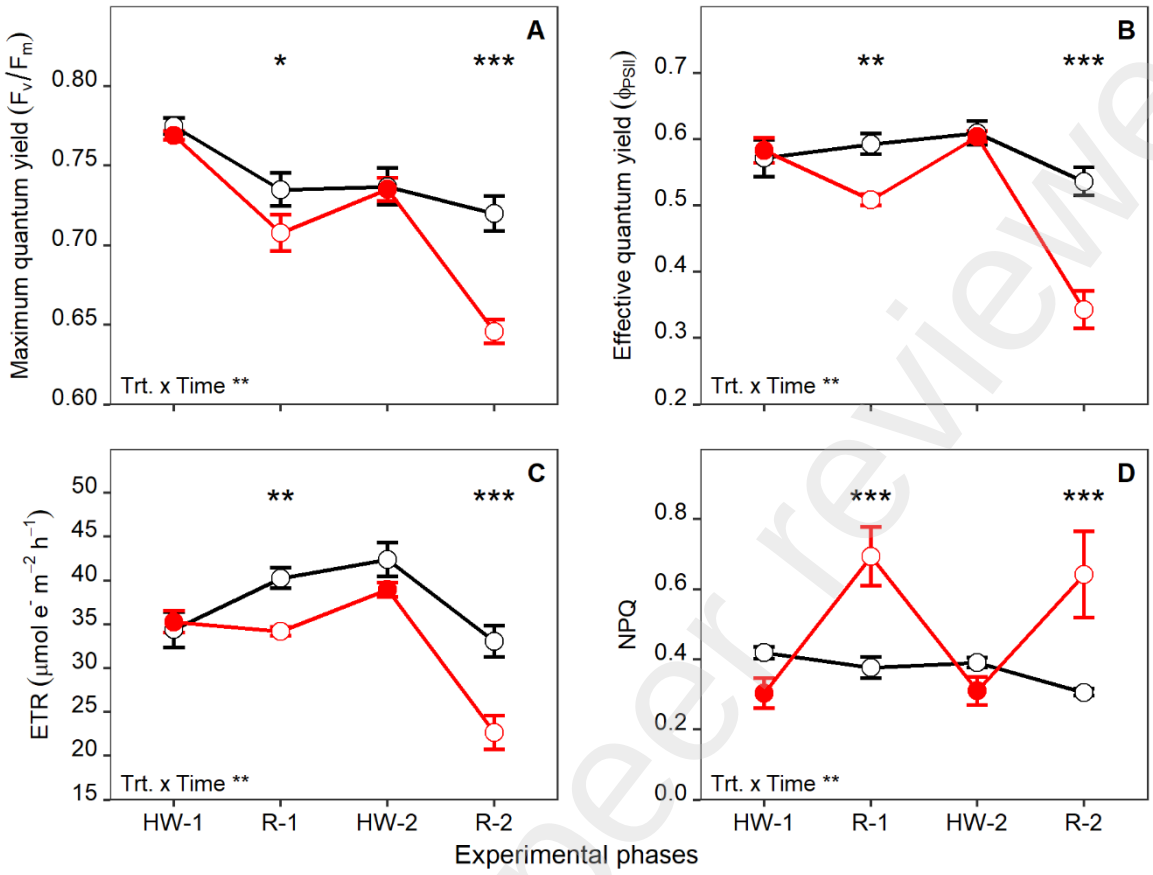

867

868 Fig. 3

Preprint not peer reviewed

This preprint research paper has not been peer reviewed. Electronic copy available at: https://ssrn.com/abstract=4489233

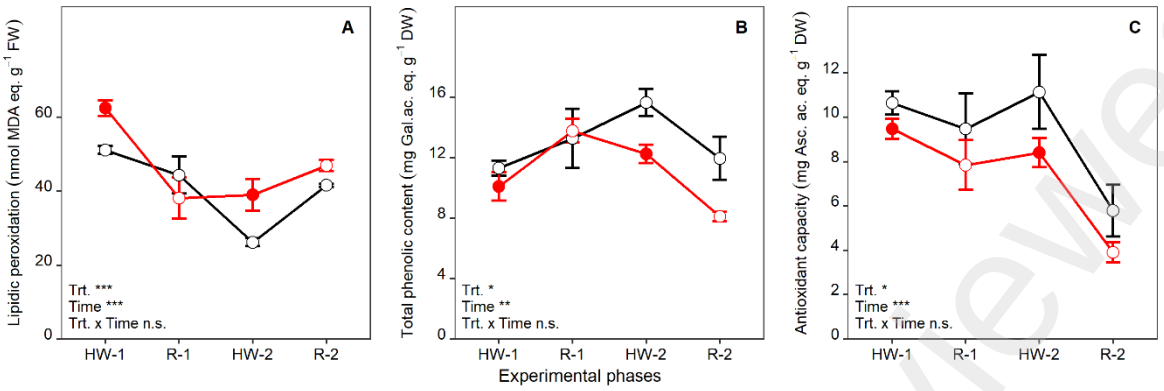

869

870 Fig. 4.

Preprint not peer reviewed

This preprint research paper has not been peer reviewed. Electronic copy available at: https://ssrn.com/abstract=4489233

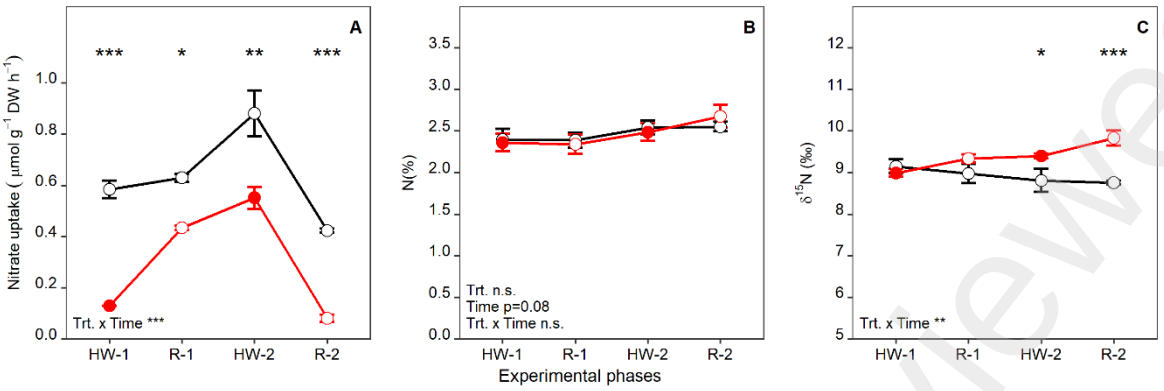

871

872 Fig. 5.

Preprint not peer reviewed

This preprint research paper has not been peer reviewed. Electronic copy available at: https://ssrn.com/abstract=4489233

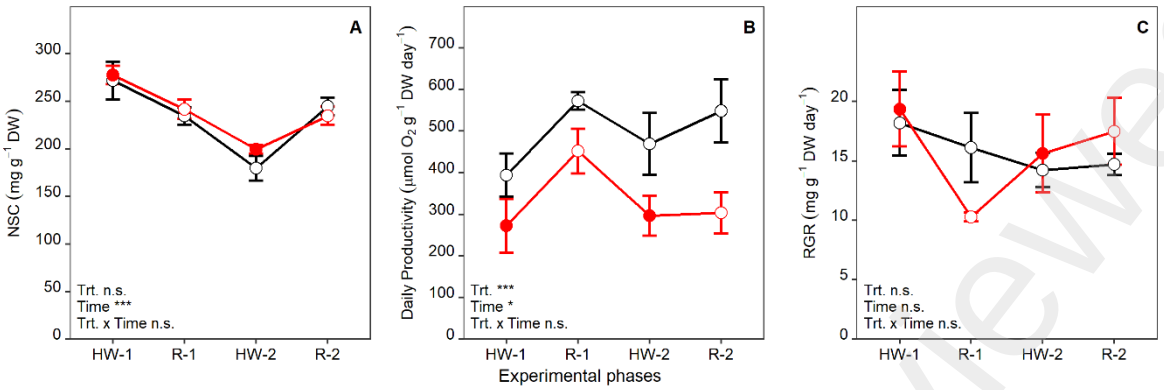

873

874 Fig. 6.

875

Preprint not peer reviewed

This preprint research paper has not been peer reviewed. Electronic copy available at: https://ssrn.com/abstract=4489233

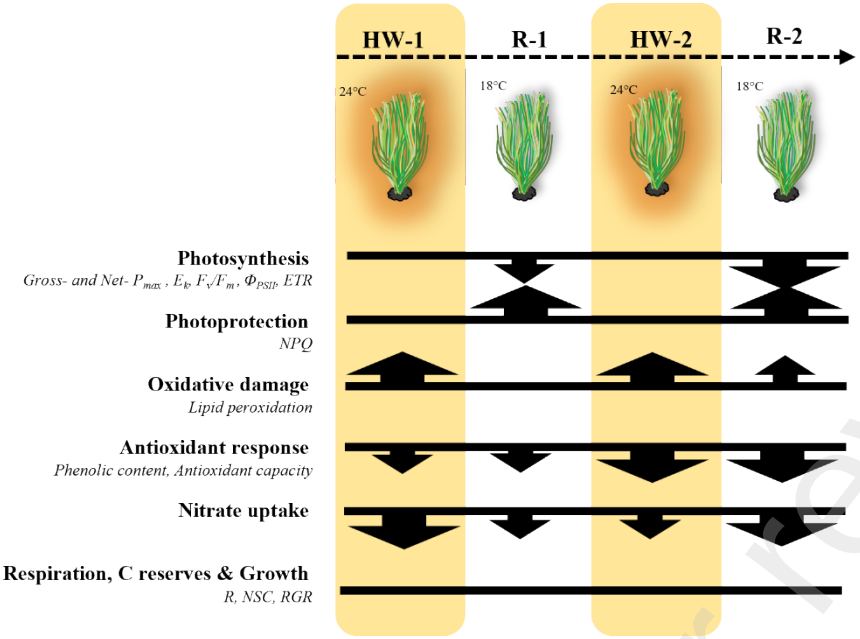

876

877 Fig. 7.

Preprint not peer reviewed

This preprint research paper has not been peer reviewed. Electronic copy available at: https://ssrn.com/abstract=4489233

9. Tables

Table 1. Permutational analysis of variance (PERMANOVA) applied to the physiological responses of *Phyllospadix scouleri* to two temperature treatments (MHWs and Control), with four sampling times (HW-1, R-1, HW-2, R-2). The treatment MHWs included two consecutive heatwaves of 24°C (HW-1 and HW-2) and their respective recovery periods at 18°C (R-1 and R-2). A reference group of plants (Control) was maintained at a constant temperature of 18°C during the experiment. In the case of paired comparisons, the Bonferroni adjustment was applied. P values in bold text indicate statistical significance at $P < 0.05$.

Main test				
Source	df	MS	Pseudo-F	P
Treatment	3	81	6	**0.001**
Time	1	87	7	**0.001**
Treatment * Time	3	41	3	**0.001**
Residuals	23	12		
Pairwise tests				
Between treatments for each sampling time				
	HW-1	R-1	HW-2	R-2
C x MHWs	0.256	0.092	0.176	**0.048**
Between sampling times for each treatment				
	C	MHWs		
HW-1 x R-1	0.330	**0.030**		
HW-1 x HW-2	0.186	**0.036**		
HW-1 x R-2	0.222	**0.012**		
R-1 x HW-2	0.498	0.204		
R-1 x R-2	2.214	0.078		
HW-2 x R-2	0.228	**0.018**		

Preprint not peer reviewed

This preprint research paper has not been peer reviewed. Electronic copy available at: https://ssrn.com/abstract=4489233